JOURNAL OF APPLIED ELECTROCHEMISTRY 22 (1992) 705–710

Preparation and properties of Raney nickel electrodes on Ni–Zn base for H_2 and O_2 evolution from alkaline solutions Part I: Electrodeposition of Ni–Zn alloys from chloride solutions

J. BALEJ*

Consultant Bureau for Chemical Engineering, Teichstrasse 9, D-5170 Jülich, Germany

J. DIVISEK, H. SCHMITZ, J. MERGEL

Research Centre (KFA) Jülich, Institute of Applied Physical Chemistry, P.O. Box 1913, D-5170 Jülich, Germany

Received 25 June 1991; revised 12 November 1991

Experimental results for the electrodeposition of Ni–Zn alloys from chloride solutions, with addition of H_3BO_3 and without other additives, in a laboratory cell with a perforated nickel sheet cathode and with recirculating electrolyte are presented. The dependence of the zinc content in the alloy on the following operating conditions was investigated: cathodic current density, 1.0–20.0 A dm^{-2}; temperature, 35–65° C; pH 1.5–5.5; total molarity, $M_{tot} = M_{Ni}^{2+} + M_{Zn}^{2+} = 1.1 - 2.8$ M; and, molar ratio, $P = M_{Ni}^{2+}/M_{Zn}^{2+} = 1.0 - 15$. Depending on the operating conditions the Zn content in the alloy varied over the range 22–88 mol %. In separate experiments galvanostatic polarization curves were measured in the direction of increasing and then decreasing cathodic current density in the range 0.1–20.0 A dm^{-2} with all other operating conditions as used for electroplating experiments. In all cases significant hysteresis effects were observed. It was found that the current efficiency for the electrodeposition of Ni–Zn alloys from chloride solutions as a function of the zinc content in the alloy showed a sharp minimum of about 55% at $X_{Zn} = 55$ mol % irrespective of other operating conditions.

1. Introduction

Raney nickel electrodes are highly suitable, not only for the cathodic evolution and anodic ionization of hydrogen [1], but also for the anodic evolution of oxygen from alkaline solutions [2–7]. Apart from aluminium, as normally used, it is also possible to use zinc as the base component of the precursor alloy. In the latter case, the precursor alloy can also be produced by electrodeposition from aqueous solutions [8, 9].

The electrodeposition of Ni–Zn alloys was studied as a typical example of the anomalous deposition of alloys [8, 9] consisting in a preferential deposition of the less noble component (i.e. zinc) under certain deposition conditions; the molar ratio of both components in the alloy ($P' = X_{Ni}/X_{Zn}$) is then lower than the corresponding molar ratio of the cations ($P = M_{Ni}^{2+}/M_{Zn}^{2+}$) in the electrolyzed solution. To explain the anomalous electrodeposition of alloys different theories have been proposed [8–13].

The electrodeposition of Ni–Zn alloys with about 10–15 wt % Ni has recently been studied with a view to producing corrosion-resistant steel plate coatings for the automotive industry [14–22]. The electrodeposition of these alloys for the production of Raney nickel electrodes with low hydrogen and oxygen overvoltage in alkaline solutions has only been dealt with in a few studies to date [23, 24]. This paper describes studies concerning the electrolytic deposition on Ni–Zn alloys with a broader concentration range (about 22–88 mol % Zn) from simple chloride solutions, with addition of H_3BO_3 and without other additives, in order to derive suitable conditions for the preparation of highly active Raney nickel electrodes for both hydrogen and oxygen evolution from alkaline solutions.

2. Experimental details

The experiments were carried out in a rectangular PVC laboratory cell with a maximum current load of 20 A and circulating electrolyte. In the central cathodic compartment, a cathode of perforated nickel sheet (VECO, effective dimensions 10 cm × 5 cm × 0.05 cm, about 40% free surface) coated additionally with a 10 μm thick layer of electrolytic nickel from a

* Present address: D-8850 Donauwörth, Johanniterstrasse 28, Germany

0021-891X/92

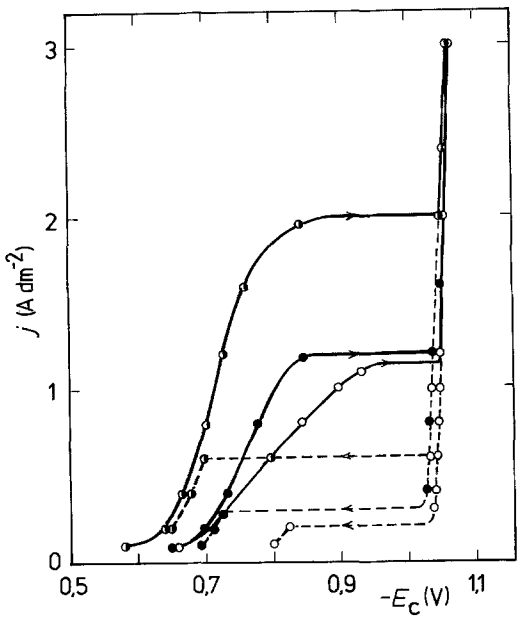

Fig. 1. Galvanostatic steady state polarization curves for the electrodeposition of Ni–Zn alloys from chloride solutions at ascending (——) and descending (– – –) current densities for various temperatures: 35° C (○); 45° C (●); 55° C (◑); (M_{tot} = 1.16 M; P = 6.8; pH 2.0).

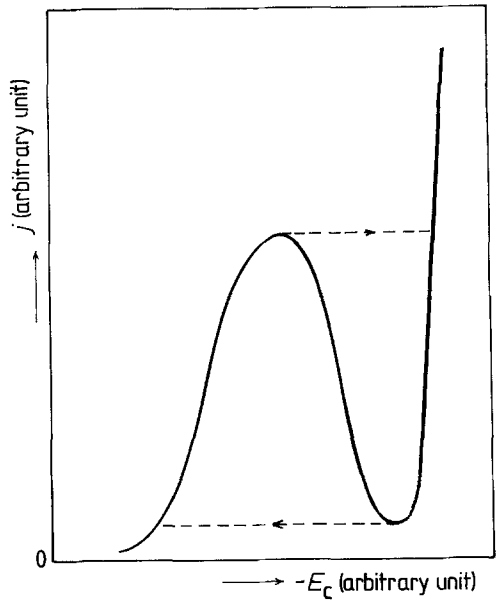

Fig. 2. Schematic potentiostatic (——) and galvanostatic (– – –) polarization curve for electrodeposition of Ni–Zn alloys from aqueous solutions.

sulphamate bath [25] was positioned vertically. It was separated from two parallel soluble anodes of nickel (99.9%) and zinc (99.5%) strip using separators of polyamide fabric. For a uniform current load on both sides of the cathode, direct current was supplied from two variable current sources connected in parallel. The potential distribution on the cathode was measured against a saturated calomel electrode (SCE) by means of adjustable Luggin capillaries. The composition, pH, temperature and flow rate of the electrolyte, as well as the cathodic current density, were kept constant at selected values (within ±2%) in individual experiments ($M_{tot} = M_{Ni}^{2+} + M_{Zn}^{2+}$ = 1.1 – 2.8 M; molar ratio $P = M_{Ni}^{2+}/M_{Zn}^{2+}$ = 1.8–14.8; pH 1.5–5.5; t = 25–65° C; 30 ± 5 wt % H_3BO_3). Mixing of the electrolyte flowing from bottom to top in the cathode compartment was enhanced by sparging with an adjustable air stream. In each experiment a constant quantity of electricity Q = 21 600 C was passed through the cell.

The soluble nickel and zinc strip anodes were immersed in the bath a few seconds prior to switching on the current and removed immediately after the deposition experiment, in order to prevent the spontaneous cementation reaction

$$NiCl_2(aq) + Zn(s) \longrightarrow Ni(s) + ZnCl_2(aq)$$

which would lead to an undesirable change in the solution composition.

In the same cell steady state galvanostatic polarization curves for the electrodeposition of Ni–Zn alloys were measured on separate, freshly prepared nickel cathodes for all individual operating conditions. The current density, in the range 0.1–20.0 A dm^{-2}, was changed stepwise, initially in the direction of increasing and then decreasing values.

Before starting, and after finishing the experiment, the whole nickel cathode (with isolated frame) was weighed in the dry state. For a representative sample of the Ni–Zn deposit, the sum of Ni + Zn was first determined complexometrically; for the same sample, the zinc content was similarly determined after the addition of 2,3-dimercaptopropanol [26]. The current efficiency for electrodeposition of the Ni–Zn alloy was calculated from the total weight of the deposit and its composition.

The Ni^{2+} and Zn^{2+} ion content in the electrolyte before and after each experiment was determined in a manner similar to that for the alloy composition. The average values of both determinations served as the characteristic solution composition for the given experiment.

3. Results and Discussion

3.1. *Galvanostatic polarization curves for the electrodeposition of Ni–Zn alloys*

A typical example of the steady galvanostatic polarization curve for the electrodeposition of Ni–Zn alloys from chloride solutions is shown in Fig. 1. In the initial stage, the polarization curve shows the usual

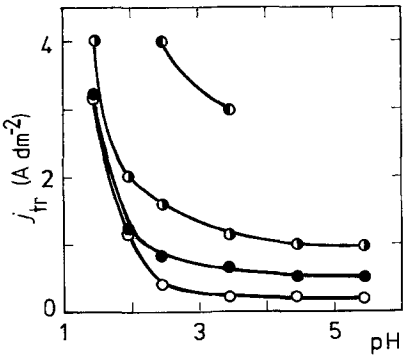

Fig. 3. Plot of j_{tr} against pH for various temperatures: 35° C (○); 45° C (●); 55° C (◑); 65° C (◐); (M_{tot} = 1.16 M; P = 6.8).

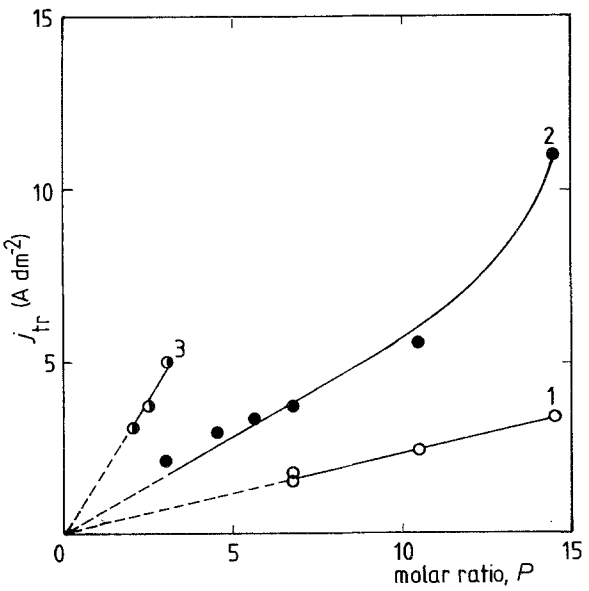

Fig. 4. Plot of j_{tr} against P for increasing current densities and various total solution molarities: M_{tot} = 1.16 (1), 1.84 (2) and 2.8 M (3) (t = 55° C; pH 3.5).

form passing over into a horizontal stage with a significant increase in the cathodic potential at constant current density. In the initial stage the electrodeposition of Ni–Zn alloy proceeded normally, i.e. with preferential deposition of nickel as a more noble component [8, 9]. Above 1000 mV/SCE a very sharp break was observed in the course of the polarization curve: only very small changes of the cathodic potential were caused by further increase in the cathodic current density up to its highest value 20 A dm^{-2} used in our measurements (not shown in Fig. 1). After reversing the current the potentials on the descending, almost vertical, part of the polarization curve agreed very well with the previous ones. However, the horizontal part appeared at a lower current density than in the ascending direction. More or less significant hysteresis effects were observed in this manner for all galvanostatic polarization curves. Such observations were not mentioned in previous papers [8, 9, 27, 28], because only polarization curves in the direction of ascending current density were measured.

The horizontal part of the polarization curve cannot be identified with the usual electrochemical diffusion limiting current density for two reasons: (i) there is always a difference in the limiting current density values in the ascending and descending directions although all other reaction conditions were kept constant; and (ii) over the whole range of current densities (0.1–20.0 A dm^{-2}) used the electrodeposition of Ni–Zn alloys was the main faradaic cathodic process usually with high current efficiency (see later), in which only the alloy composition changed with changing electrode potential. Therefore, the pseudo-limiting current densities with marked hysteresis are denoted as transition current densities in this paper, in accordance with [9]. Potential change to more negative values in the transition region is accompanied by a significant increase in zinc content. Hence, alloys deposited at the same transition current densities may differ quite profoundly in composition from each other.

The occurrence of hysteresis in the galvanostatic polarization curves can be explained by comparing them with the potentiostatic polarization curve for the same process [29] (schematically shown in Fig. 2) which exhibits the typical S-shape of an inhibited electrode reaction and proceeds reproducibly in both directions without hysteresis.

Some dependencies of the transition current densities on other reaction parameters were also observed, and some examples are presented. In Fig. 3, a significant decrease in the transition current density may be seen with increasing pH, especially in the range 1.5–2.5, at all temperatures. Figure 4 shows a linear relationship between the transition current density and molar ratio P in the range $j_{tr} < 5$ A dm^{-2} for all three total solution molarities, M_{tot}. The results of Figs. 3 and 4 relate to transition current densities in the direction of increasing current densities; similar dependencies were

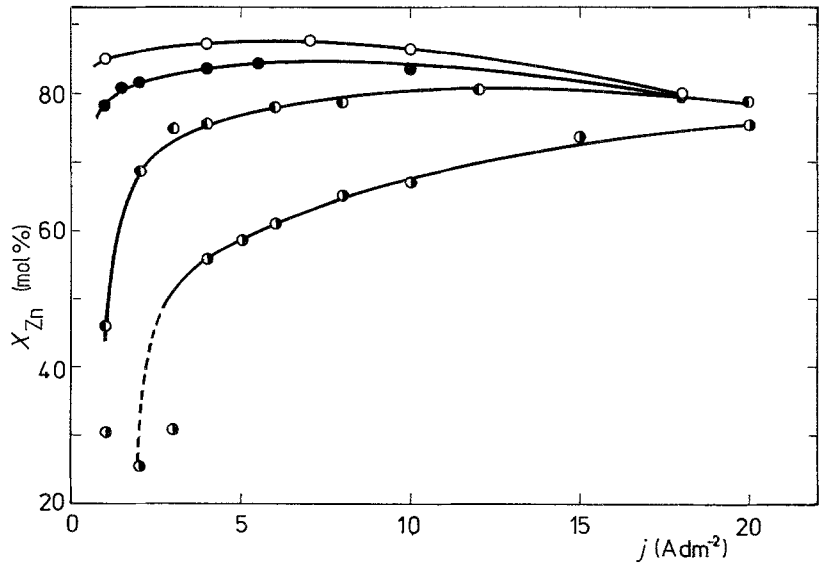

Fig. 5. Plot of X_{Zn} against current density at different temperatures: 35° C (○); 45° C (●); 55° C (◐); 65° C (◑) (M_{tot} = 1.16 M; pH 3.5; P = 6.8).

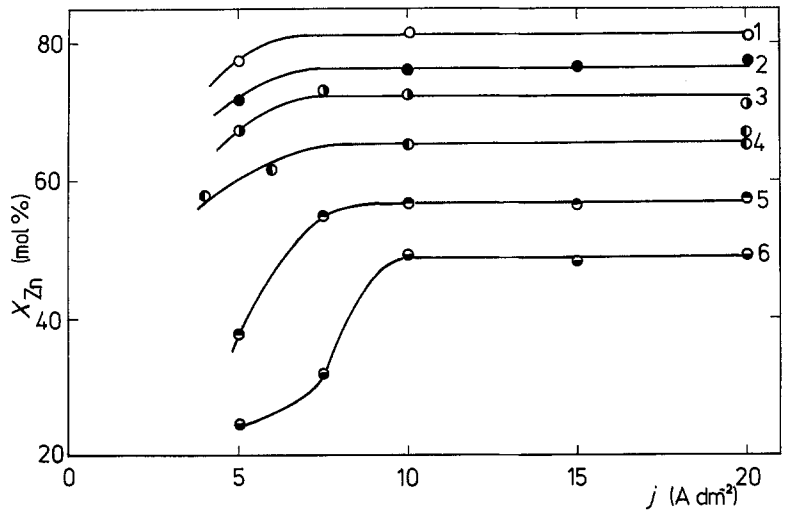

Fig. 6. Plot of X_{Zn} against current density at different molar ratios (P): 3.0 (1); 4.5 (2); 5.6 (3); 6.8 (4); 10.5 (5); 14.5 (6); (M_{tot} = 1.83 M; pH 3.5; t = 55° C).

also found for transition current densities in the reverse direction. Change in electrolyte flow rate as well as air flow were without major effect.

3.2. *Composition of Ni–Zn electrodeposits as a function of individual reaction parameters*

The influence of the current density (in the range j_c = 1.0–20.0 A dm^{-2}) on the alloy composition X_{Zn} (mol %) at 35, 45, 55 and 65° C with other parameters kept constant (M_{tot} = 1.16 M, P = 6.8, pH 3.5, electrolyte flow rate V_{sol} = 7.4 dm^3 min^{-1}, flow rate of sparge-air, V_{air} = 3.0 dm^3 min^{-1}) is shown in Fig. 5. It can be seen that, even at the lowest current densities used (j_c = 1–2 A dm^{-2}), the alloy composition lay in the transition region corresponding to the transition current densities at 55 and 65° C or even beyond this region at 35 and 45° C. With increasing current density the zinc content in the alloy increased to a 'flat' maximum (at 35–55° C) after which it began to decrease slowly. At 65° C, the maximum zinc content was not attained within the range of current densities used. The maximum zinc content in the alloy decreased with increasing temperature, while the current density necessary for maximum zinc content increased at an elevated temperature. Figure 5 also clearly shows that the influence of temperature on the alloy composition is greatest at low current densities and decreases as these increase so that, under identical conditions, it is almost negligible at j_c = 20 A dm^{-2}.

Figure 6 shows the dependence of the alloy Zn content on the current density for different molar ratios, P, of both cations in the electrolyte with higher total concentration, M_{tot} = 1.84 M, and with other parameters kept constant. In this case, the zinc content, after its initial increase, remained unchanged at its maximum value with further increase in current density up to its highest value, 20 A dm^{-2}. As expected, the Zn content of the alloy decreased with increasing P, i.e. with increasing M_{Ni}^{2+} and simultaneously decreasing M_{Zn}^{2+}.

Similar results were also found for the electrodeposition of Ni–Zn alloys from more concentrated solutions with M_{tot} = 2.8 M (not shown in detail here). Figure 7 depicts the correlation between the maximum attainable alloy content for zinc (for the given solution composition and appropriate current

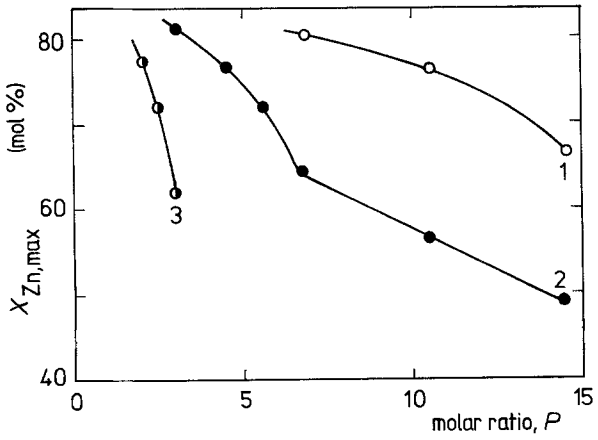

Fig. 7. Plot of X_{Zn} against molar ratio (P) for various total solution molarities: M_{tot} = 1.16 (1); 1.83 (2) and 2.8 M (3) (t = 55° C; pH 3.5).

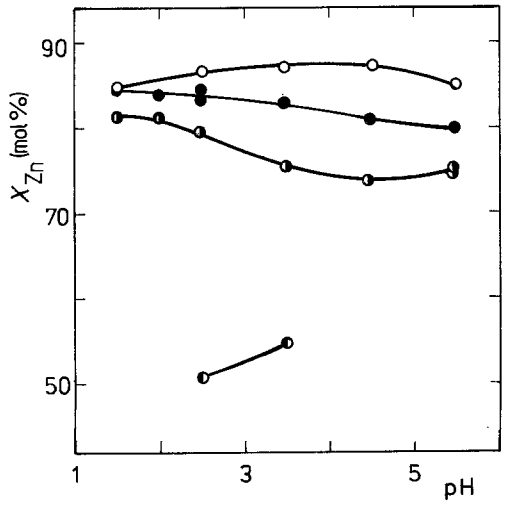

Fig. 8. Plot of X_{Zn} against pH for various temperatures: 35° C (○); 45° C (●); 55° C (◑); 65° C (◐) (M_{tot} = 1.16 M; P = 6.8; j_c = 4.0 A dm^{-2}).

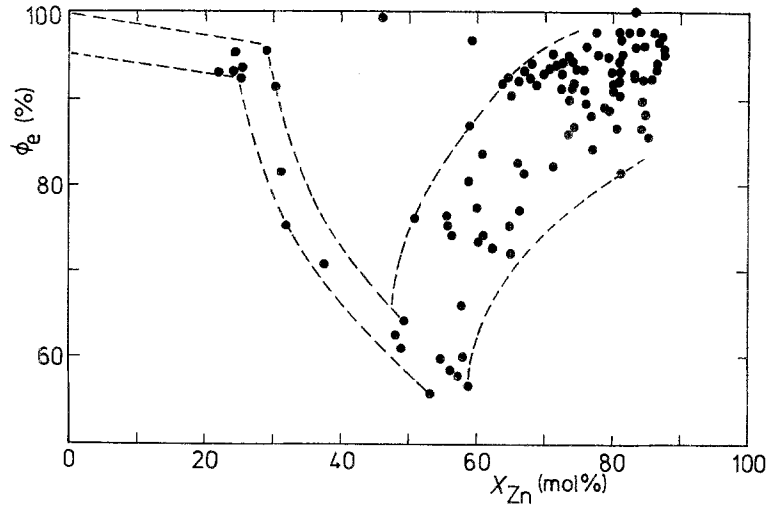

Fig. 9. Plot of current efficiency ϕ_e against X_{Zn} for individual operating conditions: M_{tot} = 1.16 (○), 1.83 (●) and 2.8 M (◑); t = 35–65° C; j_c = 1–20 A dm^{-2}, pH 1.5–5.5.

density range) and the molar ratio, P, in the solution for three different values of M_{tot} at 55° C and pH 3.5. It may be concluded from Fig. 7 that for a given alloy composition, e.g. in the range 60–80 mol % Zn, a correspondingly lower molar ratio of the two metal cations in the solution must be arranged for deposition from more concentrated solutions. It can be seen for M_{tot} = 1.84 M that the generally non-linear relation between X_{Zn} and P for X_{Zn} < 65 mol % changes to a linear relation in the range X_{Zn} > 65 mol %. This change is probably attributable to a change in the structure of the electrodeposit (silvery surface with very fine cracks at X_{Zn} < 65 mol % and a light grey surface at X_{Zn} > 65 mol %).

Earlier solubility measurements in the system $NiCl_2$–$ZnCl_2$–H_3BO_3–H_2O [30] have shown that the total concentration in saturated solution, for example at 15° C it is M_{tot} = 6.0 to 4.2 M in the broad range of P = 1–15, i.e. far above the highest total concentration value of M_{tot} = 2.8 M used. The use of such high concentrations would therefore permit higher current densities so as to shorten the production process. Certain orientation tests with M_{tot} > 3.5 M and correspondingly high current densities have shown, however, that the adhesive strength of the coating deposited on the nickel substrate deteriorates without further additives. For these reasons, no further experiments were carried out with solutions of higher concentration.

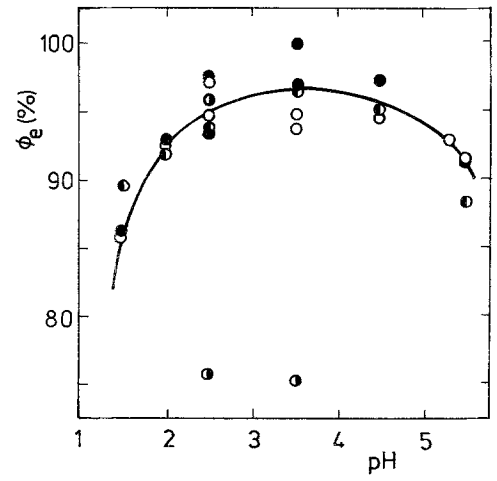

Fig. 10. Plot of current efficiency ϕ_e pH for 35 (○), 45 (●), 55 (◐) and 65° C (◑) at other operating conditions: M_{tot} = 1.16 M; P = 6.8; j_c = 4.0 A dm^{-2}.

Variation of pH in the range 1.5–5.5 shows a small influence on X_{Zn} which does not vary uniformly at different temperatures (see Fig. 8). Since acid solutions enhance the spontaneous corrosion of soluble anodes, whereas sparingly soluble hydroxides of the two metal cations can be precipitated at pH ~ 6.5, the optimum pH lies between 3 and 4.

The volumetric flow rate of the electrolyte in the range V_{sol} = 3.8–7.4 dm^3 min^{-1} as well as additional air sparging (V_{air} = 0–3.0 dm^3 min^{-1}) influenced the zinc content in the deposit slightly. At M_{tot} = 1.16 M, pH 3.5, t = 55° C, j_c = 10 A dm^{-2} and V_{air}, for example, the zinc content changed from 79.4 mol % at V_{sol} = 3.8 dm^3 min^{-1} to 81.2 mol % at V_{sol} = 7.4 dm^3 min^{-1}. Additional air sparging with V_{air} = 3.0 dm^3 min^{-1} did not affect the zinc content further.

3.3. *Current efficiencies for the electrodeposition of Ni–Zn alloys*

Figure 9 shows a sharp minimum in the current efficiency ϕ_e = 55% at X_{Zn} = 55 mol % despite the large scatter of data caused by individual deposition conditions varying over broad ranges. This clearly indicates that the current efficiency is primarily determined by the zinc content in the deposited alloy, whereas other parameters play a minor role. From Fig. 10, depicting the effect of pH on the current efficiency, an optimum at pH 3.5, independent of temperature, may be deduced. It may further be assumed that other parameters have a limited influence, but this was not further pursued within the scope of the present studies.

Current efficiencies below 100% are caused by simultaneous hydrogen evolution accompanied by a corresponding pH increase in the vicinity of the cathode. The observed minimum in the current efficiency (Fig. 9)

may be explained by a minimum in the hydrogen overvoltage on alloys with $X_{Zn} \simeq 55$ mol %. A current efficiency minimum as a function of alloy composition has also been observed by other authors [27, 31–33].

The results for the dependence of the composition of Ni–Zn alloys on individual deposition conditions are in good qualitative agreement with those of other authors (for a survey see [8, 9]). They are also consistent with the hydrogen suppression mechanism of the anomalous deposition of Ni–Zn alloys [9], which is simultaneously facilitated by alloy formation with extremely low zinc activity [34].

References

[1] E. W. Justi and A. W. Winsel, 'Kalte Verbrennung – Fuel Cells', F. Steiner Verlag, Weinheim (1962).
[2] J. Divisek, H. Schmitz and J. Mergel, *Chem.-Ing.-Tech.* **52** (1980) 465.
[3] J. Divisek, J. Mergel and H. Schmitz, *Int. J. Hydrogen Energy* **7** (1982) 695.
[4] J. Divisek and H. Schmitz, *ibid.* **7** (1982) 703.
[5] J. Balej, *ibid.* **10** (1985) 89.
[6] V. Plzak and H. Wendt, *Chem.-Ing.-Tech.* **58** (1986) 415.
[7] J. Divisek, J. Mergel and H. Schmitz, *Int. J. Hydrogen Energy* **15** (1990) 105.
[8] A. Brenner, 'Electrodeposition of Alloys: Principles and Practice', Vol. II, Academic Press, New York (1963) pp.194–238.
[9] D. E. Hall, *Plat. Surf. Finish.* **70** (1983) 59.
[10] B. P. Yur'ev, Trudy Leningrad. Politekh. Inst., No. 223 (1963) 87.
[11] H. Dahms and J. Croll, *J. Electrochem. Soc.* **112** (1965) 771.
[12] D. M. Kolb, M. Przasnyski and H. Gerischer, *J. Electroanal. Chem.* **54** (1974) 25.
[13] M. J. Nicol and H. I. Philip, *ibid.* **70** (1976) 233.
[14] R. G. Baker and C. A. Holden, *Plat. Surf. Finish.* **72** (1985).
[15] L. D. Vater, *Metalloberfläche* **43** (1989) 201.
[16] H. Kammereck, J. Sievert, F. Weber and H. U. Weigel, *Stahl und Eisen* **109** (1989) 295.
[17] L. Felloni, R. Fratesi, F. Quadrini and G. Roventi, *J. Appl. Electrochem.* **17** (1987) 574.
[18] H. Fukukshima, T. Akiyama, K. Higashi, R. Kammel and M. Karimkhani, *Metall* **42** (1988) 242.
[19] W. Siegert and J. Hadley, *Metalloberfläche* **43** (1989) 78.
[20] R. Albalat, E. Gómez, C. Müller, M. Sarret, E. Vallés and J. Pregonas, *J. Appl. Electrochem.* **20** (1990) 635; 21 (1991) 44.
[21] M. F. Mathias and T. W. Chapman, *J. Electrochem. Soc.* **137** (1990) 102.
[22] M. J. Mathias, C. M. Villa and T. W. Chapman, *J. Appl. Electrochem.* **20** (1990) 1.
[23] K. Sasaki and K. Sugiyama, *Kogyo Kogaku Zasschi* (1957) 387.
[24] I. Paseka and J. Balej, *Chem. Prum.* **20** (1970) 305.
[25] F. A. Lowenheim, 'Modern Electroplating', 3rd ed., J. Wiley & Sons, New York (1974) p.314.
[26] E. Merck, Kompexometrische Bestimmungsmethode mit Titriplex. E. Merck, Darmstadt.
[27] Y. Imai and M. Kurachi, *Denki Kagaku* **45** (1977) 728.
[28] B. P. Yur'ev and L. V. Volkov, *Zh. prikl. khim.* **38** (1985) 66; *J. Appl. Chem. USSR* **38** (1965) 61.
[29] J. Mindowicz, C. Capel-Boute and C. Decroly, *C.R. Acad. Sci.* **256** (1963) 148.
[30] J. Balej, *J. Chem. Soc., Faraday Trans. 1.*, **85** (1989) 3327.
[31] T. L. Rama Char and S. K. Panikkar, *Electroplat. & Metal Finish.* **13** (1960) 405.
[32] N. A. Marchenko and Zh. v. Batyuk, *Zh. prikl. khim.* **37** (1964) 595; *J. Appl. Chem. USSR* **37** (1964) 599.
[33] M. Kurachi and K. Fujiwara, *Denki Kagaku* **38** (1970) 600.
[34] Y. Imai, T. Watanabe and M. Kurachi, *ibid.* **46** (1978) 202.